



Published in final edited form as:

*Int J Rock Mech Min Sci* (1997). 2015 October ; 79: 9–18. doi:10.1016/j.ijrmms.2015.08.001.

## Analysis of gob gas venthole production performances for strata gas control in longwall mining

C. Özgen Karacan

NIOSH, Office of Mine Safety and Health Research, Pittsburgh, PA 15236, United States

### Abstract

Longwall mining of coal seams affects a large area of overburden by deforming it and creating stress-relief fractures, as well as bedding plane separations, as the mining face progresses. Stress-relief fractures and bedding plane separations are recognized as major pathways for gas migration from gas-bearing strata into sealed and active areas of the mines. In order for strata gas not to enter and inundate the ventilation system of a mine, gob gas ventholes (GGVs) can be used as a methane control measure. The aim of this paper is to analyze production performances of GGVs drilled over a longwall panel. These boreholes were drilled to control methane emissions from the Pratt group of coals due to stress-relief fracturing and bedding plane separations into a longwall mine operating in the Mary Lee/Blue Creek coal seam of the Upper Pottsville Formation in the Black Warrior Basin, Alabama. During the course of the study, Pratt coal's reservoir properties were integrated with production data of the GGVs. These data were analyzed by using material balance techniques to estimate radius of influence of GGVs, gas-in-place and coal pressures, as well as their variations during mining.

The results show that the GGVs drilled to extract gas from the stress-relief zone of the Pratt coal interval is highly effective in removing gas from the Upper Pottsville Formation. The radii of influence of the GGVs were in the order of 330–380 m, exceeding the widths of the panels, due to bedding plane separations and stress relieved by fracturing. Material balance analyses indicated that the initial pressure of the Pratt coals, which was around 648 KPa when longwall mining started, decreased to approximately 150 KPa as the result of strata fracturing and production of released gas. Approximately 70% of the initial gas-in-place within the area of influence of the GGVs was captured during a period of one year.

### Keywords

Pratt coal; Upper Pottsville Formation; Longwall mining; Methane control; Gob gas ventholes; Coal gas; Material balance

---

Correspondence to: C. Özgen Karacan.

Disclaimer: The findings and conclusions in this paper are those of the author and do not necessarily represent the views of the National Institute for Occupational Safety and Health (NIOSH). Mention of any company name, product, or software does not constitute endorsement by NIOSH.

## 1. Introduction

Longwall mining induces deformation, fracturing, and bedding plane separations within a large volume in the overburden strata. These effects can release a significant amount of gas from overburden strata, which may find its way into sealed and active areas of the mine if not controlled. Therefore, strata gas control, especially in geologies with high gas amount, is an important consideration in support of ventilation to ensure mine safety in addition to its benefits as an unconventional energy source.<sup>1–3</sup>

In the U.S and elsewhere, gob gas ventholes (GGVs) are the most common borehole type used to control gas from the fractured strata by capturing it before it can enter the mine environment.<sup>4–8</sup> Despite the importance of these boreholes in controlling gob gas, it may be hard to predict their performance due to stability issues,<sup>9,10</sup> relative importance of different operational parameters on their performance,<sup>11</sup> and the effect of surface elevation (overburden thickness) on the rate-decline properties.<sup>12</sup> A schematic representation of the various zones of deformation in longwall overburden and a GGV placed to control strata gas is shown in Fig. 1.

While some of the operational constraints, such as suction pressure, casing depth, proximity to tailgate of the longwall panel, can be addressed for optimum performance of GGVs,<sup>11</sup> one of the most important aspects of gob gas venthole performance is dynamic subsidence and the geology of the overburden strata that is affected by it. Dynamic subsidence, or surface movement, of a particular location begins as mining face approaches, and continues until maximum displacement occurs after longwall face passes that location to some distance. The magnitude of the displacement and how it progresses are controlled primarily by the thickness of the extraction, the width of the panel, the overburden thickness and the properties of the strata. The properties of the strata not only affect the subsidence and the stress distribution,<sup>13</sup> but also where emission potential from the strata surrounding the coal mine can develop and how GGV designs can be optimized to control emissions. Without well-developed permeable paths, GGVs may not be effective at all. Therefore, the location of GGVs and completion intervals are decided in relation to gas sources and mining-induced fractures and bedding plane separations to be able to control strata gas. For instance, with these considerations, in the Southwestern Pennsylvania section of the Northern Appalachian basin, the GGVs of supercritical panels are traditionally located near the tailgate, or headgate, margins of the longwall panels to take advantage of tensional fractures at the panel margins to capture the methane.<sup>3</sup>

Stress-relief fractures and bedding plane separations (Fig. 1) created as the result of mining-induced deformations are the major pathways for gas migration from gas-bearing strata. Thus, in order to be able to take full advantage of the benefits of GGVs for controlling gas, zones of strata deformations should be known. Extensive effort has been made to locate fracture and strata separation intervals. An empirical method proposed by Palchik<sup>14,15</sup> is based on correlation of the presence and absence of estimated horizontal fractures with uniaxial compressive strength and thickness of rock layers, distances from the extracted coal seam to the rock layer interfaces, and the thicknesses of extracted coal. He predicted that the probability of fracturing increased with the compressive strength difference between

neighboring rock layers, i.e. weak-strong layer transitions. However, this does not mean that every single weak-strong layer interface is prone to separations. Whittles et al.<sup>16</sup> conducted studies on the effect of different geotechnical factors on characteristics of fracturing, gas sources, and gas flow paths for longwall operations in the United Kingdom. More recently, Karacan and Olea<sup>17</sup> predicted the potential intervals of strata separations using continuous wavelet transform (CWT) and generalized quadratic variations of well logs. The CWT matrix of coefficients was analyzed to locate the frequency and space parameters of singularities, which are precursors for discontinuities and weaknesses in the strata that are precursors for separation. Singularities were then isolated at their corresponding depth locations and modeled to determine their continuity and spatial correlation using single normal equation simulation (SNE-SIM). Results showed that the predicted intervals of strata separations were consistent with the expected locations of strata separations and data in the literature.

The productivity of GGVs and their rate decline behavior can be a function of complexity of the gob at the production interval, but more importantly can be a function of the magnitudes of fracture conductivity therein. Guo et al.<sup>18</sup> reported with a detailed study that in the fractured zone, vertical or sub-vertical and horizontal fractures are both well-developed and interconnected through the layers. In the deformation zone above the fractured zone, whose thickness is suggested to be between 80 m and 135 m, permeability development through strata separations is more prominent. These separations generally have very high conductivity for fluid flow, as demonstrated by Karacan and Goodman,<sup>19</sup> who determined by using well test techniques that a strata separation with a fracture thickness of 0.16 m can have a permeability of ~80 Darcy, while the effective average of the rest of the fractured gob interval could have permeability values varying between 1 and 15 Darcy,<sup>20</sup> although lesser values were observed too.<sup>21,22</sup> These are significant values for potential gas flow within the gob and between active and sealed portions of the mine, if strata separations and fractures intercept gas sources within the zone affected from the mining stresses. Strata separations and the values of fluid conductivity are not restricted only to panel areas. Gale<sup>23</sup> simulated rock fracture, caving, stress redistribution, and induced hydraulic conductivity enhancements around longwall panels, and concluded that horizontal conductivity can be significantly enhanced along bedding planes within and outside the panel area, thereby increasing the potential of methane migration from affected regions. These results are consistent with the drainage radius estimates, which go beyond the physical widths of the longwall panels, obtained using well test techniques reported in the literature herein.

Despite the advances in understanding strata geomechanics and production behavior of GGVs, some of the barriers toward effective management of methane in mines through the use of gob gas ventholes still exist due to the complexity of the gob environment, the involvement and interdependence of multiple influential factors, and the lack of knowledge on interactions of the GGV with the gob reservoir. Improvements in GGV production performance evaluation capabilities for site-specific mining conditions and circumstances can address a variety of longwall gas emission issues, resulting in improvements in GGV design and gas capture from overburden strata.

In this paper, we analyze production performances of the GGVs drilled over a longwall panel operating in the Mary Lee/Blue Creek seam of the Black Warrior basin in Alabama, to control methane emissions from the Pratt group of coals due to stress-relief fracturing and bedding plane separations. During the course of the study, Pratt coal's reservoir properties were integrated with production data of the GGVs. Then, material balance techniques were used to estimate the radius of influence of GGVs, gas-in-place, and coal pressures, as well as their variations during mining.

## **2. Background information on the location of the study area, its geology, and methane control activities**

### **2.1. Site description and analyses conducted on vertical and Horizontal degasification boreholes of the area**

The study area, which is approximately 50 km<sup>2</sup>, is located between Brookwood and Oak Grove fields in the Alabama section of the Black Warrior basin and is nearly 3 km from the main thrust fault (Figs. 2 and 5). There are multiple faults and fractures within the study area and in the basin, in general. This structural deformation have significant effect on the performance of coalbed methane wells, mining emissions, the hydrodynamics in the area, and on the pressure gradients within the coal reservoirs with varying distance to these deformations.<sup>24–26</sup>

The majority of the coal-bearing strata of economic value in the Black Warrior basin are in the Pennsylvanian age Upper Pottsville Formation. In the Upper Pottsville Formation, the Pratt, Mary Lee, and Black Creek coal groups are probably the most important ones due to mining and coal gas production activities (Fig. 3). All of these coal groups have multiple coal seams of varying thicknesses. However, the Mary Lee coal group, which covers an interval of about 75 m thickness and includes the New Castle, Mary Lee, and Blue Creek and Jagger seams is particularly important as longwall mining occurs in this coal group (Fig. 3). In the Mary Lee group, the Mary Lee and Blue Creek seams merge into a single thick unit in the Southeastern part of the basin and this unit is separated by a parting layer. During coal mining, the Mary Lee and Blue Creek seams are usually mined together. In the study area, the New Castle seam is at most 20 m and the Jagger seam is at most 13 m above and below the mining interval, respectively. The immediate consequences of stratigraphy and of the interval thicknesses between the New Castle, Mary Lee/Blue Creek, and Jagger seams are potential emissions from roof and floor through mining-induced fractures that need to be handled by the ventilation system of the mine.

Due to high gas contents and high methane emission potential into mines, as well as economic gas production, degasification of the Pratt, Mary Lee, and Black Creek coal groups was started as early as 1987, initially with ninety-two vertical boreholes in the study area (Fig. 2). Some of these boreholes were completed in five-twenty coal seams in these coal groups. Only eleven of these wellbores were completed only in the Pratt and Black Creek groups. The remaining eight-one vertical boreholes had completions also in the Mary Lee coal group, which also contains Blue Creek coal. In total, twenty of these vertical wells

had completions in the Pratt group. Most of the vertical boreholes remained in production from the 1990s until 2010–2011 for about 6000 days.

A detailed description of degasification activities in the area and a production history matching study of these boreholes to determine reservoir properties of the Pratt, Mary Lee, and Black Creek coal is presented in.<sup>27</sup> That work discussed initial reservoir properties of these coal groups, estimated the changes during the course of degasification duration until 2011 and presented the results. The coal reservoir properties of the Mary Lee coal group at different locations determined through production history matching were later used to compute time-lapsed spatial methane quantity in the New Castle, Mary Lee/Blue Creek, and Jagger seams within the mine area shown in Fig. 2 by employing filter-based multiple point geostatistical simulations.<sup>28</sup>

With the start of longwall mine planning and associated gate-road development in Blue Creek seam, horizontal in-seam bore-holes were also drilled only into the Blue Creek coal (Fig. 2). Production data analyses of in-seam horizontal wells and geostatistics for the spatial distribution of gas-in-place (GIP) were also integrated into<sup>28</sup> to assess the overall methane quantity remaining in the Blue Creek coal.<sup>29</sup> As the longwall operation progressed, vertical boreholes within panel areas were progressively terminated and some of them were converted to GGVs.

This study was conducted on the Pratt group of coals, which include Pratt seams and Curry and Gillespy seams that are believed to be the source of strata gas in this area, and on the productions of GGVs drilled to capture it.

## 2.2. Strata gas control and gob gas ventholes (GGV)

In November of 2009, the coal mine located within the study area started longwall panel extraction with the E-1 panel, which was 260 m wide and 3700 m long, to mine the Blue Creek and Mary Lee seams which are at an average depth of 473 m at the panel location. The panel was completed at the end of October, 2010. The monthly averaged daily linear advance day was 11 m/day, with a maximum of 16.7 m/day and minimum of 4.4 m/day during the entire mining period (Fig. 4). The minimum advance-rate values corresponded to the start and end of the mining. In the absence of measured data, it is not clear how dynamic deformation, i.e. strata deformations as longwall face was still affecting a particular location, progressed in the overburden during mining. However, rate of face advance is considered as one of the main factors influencing the dynamic deformation process; thus regulating the face advance rate in longwall mining was proposed as an effective means of reducing the disturbance potential to surface structures associated with the subsidence process.<sup>30</sup> Therefore, advance rate may also impact strata deformation and on the enhancement of hydraulic conductivity around gob gas boreholes.<sup>22</sup>

Although previous degasification activities using vertical and in-seam boreholes helped to reduce emissions from the Mary Lee group of coals, GGVs were also drilled along the panel to control strata gas that originates primarily from the Pratt group of coals, which are at a depth of ~275 m at the panel location. An interval thickness of 200 m between the Pratt and Mary Lee groups ensures that Pratt seams will not be in close proximity to the caved zone of

the E-1 panel. However, they can be intercepted by vertical and horizontal fractures due to stress-relief fracturing. In fact, a study based on the well logs of this area inferred that there will be bedding plane separations and horizontal fractures in Pratt coals and in the shale-sandstone transitions in deeper sections.<sup>17</sup> In order to control the gas that may be released in these zones and migrate towards the mine through fractures and bedding plane separations, six GGVs were drilled along the E-1 panel at different locations from panel start and from the tailgate (Fig. 5). In addition to the wells that were originally drilled as GGVs, a conventional CBM well (15676- C) that was perforation-completed in 2008—through a 20-cm production casing at the Pratt (256 m–289 m), Mary Lee (451 m–479 m), and Black Creek (536 m–615 m) coal zones, and with an open hole between 724 m and 759 m, and produced methane until mining started—was terminated during mining and converted to a GGV after mining was completed at the panel.

Fig. 5 shows that the locations of these GGVs at this mine site are different than those of the ones drilled at mine sites operating in the Pittsburgh coal seam in the Northern Appalachian basin. For instance, in the Southwestern Pennsylvania section of the Northern Appalachian basin, the GGVs are traditionally located near the tailgate, or headgate, margins of the longwall panels and completed very close to the caved zone with ~60 m slotted casing at the bottom.<sup>31</sup> This design is based on the close proximity of the Sewickley coal – one of the main sources of strata gas – to the Pittsburgh coal seam and to take advantage of tensional fractures at the panel margins to capture the methane with the help of vacuum pumps at variable gas quality.<sup>3</sup> However in the current study site, the source of strata gas is the Pratt group of coals, which is gassier and is approximately 200 m above the Mary Lee seams. Considering the location of the gas source and the major strata separation intervals, GGVs are mostly located close to the middle of the panels to take advantage of the bedding plane separations as flow paths under maximum stress relief. The wells are drilled to the top of the Mary Lee coal group, but are completed with a solid production casing set just above the Pratt group of coals (Fig. 6). The interval between the Pratt and Mary Lee groups is left open hole to capture any gas that may be originating from Pratt coals as well as from Curry and Gillespy coals. The combined thickness of the Pratt group of coals in the study area is around 5.2 m based on geophysical logs. These GGVs produce high-quality methane without contamination from ventilation air and flow with coal gas pressure. The produced gas is transported by a pipeline as energy source for home and industrial use.

Table 1 shows GGV well permit numbers, their locations on the panel, and completion depths. Fig. 6 presents well completion schematics to show the coal intervals covered, with relevant information related to casing sizes and setting depths.

### 2.3. Gob gas venthole (GGV) productions

Fig. 7 shows average daily methane production rates of GGVs and their change during mining of the E-1 panel and after it was completed. The wells started producing methane when the longwall face was close to their location and they all produced high-quality methane, with a specific gravity of 0.565.

The 24-hours-long flow tests conducted through an orifice during production periods of these GGVs indicated high flow rates and flowing casing pressures. The results of the flow



tests are given in Table 2. These results show that the GGVs produced with rates between  $26.2 \times 10^3 \text{ m}^3/\text{day}$  and  $54.9 \times 10^3 \text{ m}^3/\text{day}$  and with flowing production casing pressures between 274 kPa and 377 kPa. It should be noted that 15676-C was tested when it was producing as a CBM well, and the pressure was not recorded. However, it was added to this table for completeness.

### 3. Analyses, results and discussion

#### 3.1. Analyses of production characteristics of E-1 panel GGVs

Fig. 7 shows that the production rate profiles of all GGVs are noticeably similar; they are characterized by initial high flow rates potentially due to mining-induced stress-relief fracturing and expected bedding plane separations. In the Upper Pottsville Formation, these potential intervals are generally concentrated around the interfaces of sandstone and limestone with shale-rich formations, within shales and especially along the Pratt coal interval, from which the GGVs are expected to capture the gas.<sup>17</sup> After mining of the E-1 panel was completed, GGVs still continued to produce high-quality methane but at lower rates. This flow behavior shows that there were still very permeable flow paths and gas availability within the strata influenced from mining even after the panel was completed.

The average daily production rates of GGVs increased quickly to peak rates of as much as  $90 \times 10^3 \text{ m}^3/\text{day}$ , and then started to decline towards lower rates as the mining face progressed. This production characteristic can be a combination of a decrease in gas amount within the area affected by strata deformation and the GGVs' drainage radii, as well as by the dynamic nature of these deformations due to changes in abutment stresses as mining progresses. Increasing abutment stresses with mining deform overlying formations, creating fractures and bedding plane separations, and thereby promoting gas release and flow.<sup>6,32</sup> As the mining face advances, stresses behind the face start to decrease and the bedding plane separations start to close, eventually lowering gas rate. This phenomenon was also observed by monitoring of casing strains in Pittsburgh coal seam mines, which served as a proxy to determine changes in bedding plane separations to test GGV production data.<sup>33,19</sup>

Fig. 7 also shows an interesting comparison between production behavior of a conventional CBM well and the GGVs. The 15676-C was a CBM well completed at three different coal groups (Pratt, Mary Lee, and Black Creek) as discussed in Section 2.2. This well started producing methane in 2008 at an initial flow rate of approximately  $5000 \text{ m}^3/\text{day}$ . The production rate declined to  $\sim 2000 \text{ m}^3/\text{day}$  in early 2010, before the well was shut down due to the mining operation approaching the Mary Lee seams. This well was subsequently converted to a GGV. When the well resumed production as a GGV just before completion of the panel, it started producing gas from deformed strata of Pratt coals at a rate of  $\sim 8000 \text{ m}^3/\text{day}$ , very close to the after-mining rates of other GGVs, and sustained that rate until the end of August of 2013. It should be noted this production rate was higher than the methane production rate achieved by this well from all coal horizons combined as a conventional CBM well, and shows the impact of stress-relief fracturing on gas availability and flow within deformed strata and the importance of controlling it.

Fig. 8A shows the methane production rate from all GGVs combined (including the after-mining period of 15676-C) and the cumulative production. Production rate from the GGVs increased with the interception of the first GGV (16106-CG) after the start of mining and reached  $\sim 250 \times 10^3 \text{ m}^3/\text{day}$  while the panel was being mined. During mining of the E-1 panel, the production rate stayed high as new GGVs came online and the existing ones were still producing at high rates. The decrease in methane production rate to  $\sim 120 \times 10^3 \text{ m}^3/\text{day}$  during this period with a subsequent increase to more than  $200 \times 10^3 \text{ m}^3/\text{day}$  is attributed to the decreasing average linear advance rate of the longwall face to 9–10 m/day during May–July 2010 (Fig. 4). A plot of average daily advance rate against methane production rate (Fig. 8B) shows the close relationship between GGV production rate and the mining rate at this site. Although these data can be site-specific, the strong apparent correlation between mining rate and methane production rates shown in Fig. 8B signifies the importance of mining rate on dynamic subsidence and associated methane release from gassy strata, as well as the enhancement of hydraulic conductivity around gob gas boreholes to capture gas more effectively. This correlation can also suggest that if there are no GGVs ready to capture the strata gas during a certain period in mining, slowing mining advance may help to reduce gas emissions from strata to aid in ventilation.

Close to the completion of the panel, the cumulative rate started to decline to  $\sim 98.8 \times 10^3 \text{ m}^3/\text{day}$  (Fig. 8A). During mining of the panel, the cumulative methane removed from deformed strata was  $\sim 51.8 \times 10^6 \text{ m}^3$  (Fig. 8A). The production from GGVs continued even three years after the completion of E-1 and while the other panels were being mined, although at a decreasing rate. The final recorded data in August 2014 showed a methane production rate of  $\sim 4 \times 10^3 \text{ m}^3/\text{day}$  and a cumulative production of  $\sim 75.5 \times 10^6 \text{ m}^3$  from these GGVs. In other words, approximately 68% of the total methane production from deformed strata was produced during mining of the E-1 panel.

In order to put the  $\sim 75.5 \times 10^6 \text{ m}^3$  gas captured by the GGVs discussed in this paper into perspective in terms of GGV productivity and its importance for controlling strata gas, cumulative productions of all CBM wells of the study area shown in Fig. 2 and studied in detail in<sup>12</sup> are referred to here. The data and the analyses of CBM productions from all ninety-two wells completed at different coal groups (Pratt, Mary Lee, and Black Creek) indicated that they produced  $\sim 900 \times 10^6 \text{ m}^3$  methane as of 2011 from these three zones over the course of more than 6000 days.<sup>12</sup> Twenty of these CBM wells, which had completions in the Pratt coal group, produced  $\sim 92 \times 10^6 \text{ m}^3$  methane only from these seams during the same period. Although slightly higher, this quantity can be considered comparable to the  $\sim 75.5 \times 10^6 \text{ m}^3$  gas produced by the GGVs of the E-1 panel from the same coals in a shorter time as the result of stress-relief fracturing of the overburden.

### 3.2. Material balance analyses of GGV productions, gas-in-place, and formation coal pressures

Material balance computations were conducted to estimate gas-in-place and the radii of investigation for each of the GGVs by using volume CBM material balance. In these computations, it was assumed that the strata gas source was the Pratt group of coal seams,



which has an average combined thickness of 5.2 m in the study area. Due to limited production data, 16113-CG was excluded from this analysis.

In order to be able to perform material balance calculations for the start of and during mining based on production data of GGVs, the initial coal reservoir properties, i.e. coal pressure and water saturation, of Pratt coals after degasification using CBM wells had to be estimated. These properties were extracted from the results of the history matching analyses of 20 CBM wells that had completions at the Pratt coal group and were reported as “existing” in 2011 in this area.<sup>12</sup> Although this date is approximately one year later than the start of mining of the E-1 panel, it is argued that the Pratt coals' average pressure and water saturation did not change considerably within this time due to the limited number of wells that were in their decline period. Therefore, the mean values of pressure and saturation for 2011 were considered as representative and were used as the average initial properties of Pratt coal at the start of mining of the E-1 panel in December 2009.

Coal thicknesses were determined from the geophysical logs of the exploration boreholes in this mining area and combined as the total Pratt thickness (5.2 m) at each well's location. In addition, average Langmuir pressure and Langmuir volume data that were reported for Pratt coals in<sup>12</sup> were used as Pratt coals' methane sorption isotherm data. Values representing Pratt seams' average initial properties for material balance calculations are presented in Table 3.

Material balance was calculated using the volumetric gas-in-place equation with the premise that production quantities resulted in a subsequent reduction of gas-in-place and coal pressure in the Pratt group of coals within the deformed strata of the drainage area. This means that this approach is applicable when pseudo-steady-state (PSS) prevails. Considering that the fractures and the bedding plane separations are very permeable and extensive, the drainage radii can be limited to the extent of these deformations and the boundaries can be felt rapidly by the GGV. Therefore, PSS is an applicable concept in this situation.

In addition, due to the deformed nature of the drainage area and highly permeable flow paths, coal pressure can equilibrate rapidly with pressure within mining-induced fractures, which can also be very close to the flowing casing pressure of the GGV. Therefore, as the first step of the material balance calculation, test pressures given in Table 2 and the cumulative methane productions corresponding to those dates were used, along with the initial conditions given in Table 3, to estimate the size of the drainage area through an approximate drainage radii of each GGV (Eq. (1)). In this equation,  $N_p$  is the cumulative gas produced until the test and  $r_e$  is the drainage radius of the zone of influence of the GGV. The subscripts “ $i$ ” and “ $n$ ” refer to the initial condition and the condition at the time of the test, respectively. After determining the drainage radius, initial gas-in-place ( $G_i$ ) for each GGV was calculated by using average initial coal pressure (648 kPa). Subsequent drops in pressure and the changes in other parameters that depend on pressure within the drainage area ( $A$ ), as well as remaining gas-in-place, were calculated by an iterative pressure estimation process matching the incremental amount of gas produced between sequential dates ( $i + 1$ ,  $i + 2$ , .....). This procedure follows PSS and the drainage area does not change once it is established, although deliverability may change. This computation scheme is

shown as Eqs. (1) and (2) and was performed for the first twelve months of GGV productions, including mining of the E-1 panel.

$$r_e = \sqrt{\frac{N_p}{h\pi \left( \left( \frac{\varphi_i(1-Sw_i)}{B_{g_i}} + \frac{V_L P_i}{P_i + P_L} \rho \right) - \left( \frac{\varphi_i(1-Sw_i)}{B_{g_n}} + \frac{V_L P_n}{P_n + P_L} \rho \right) \right)}} \quad (1)$$

$$G_i - G_{i+1} = Ah \left[ \left( \frac{\varphi_i(1-Sw_i)}{B_{g_i}} + \frac{V_L P_i}{P_i + P_L} \rho \right) - \left( \frac{\varphi_i(1-Sw_i)}{B_{g_{i+1}}} + \frac{V_L P_{i+1}}{P_{i+1} + P_L} \rho \right) \right]$$

$$G_{i+1} - G_{i+2} = Ah \left[ \left( \frac{\varphi_i(1-Sw_i)}{B_{g_{i+1}}} + \frac{V_L P_{i+1}}{P_{i+1} + P_L} \rho \right) - \left( \frac{\varphi_i(1-Sw_i)}{B_{g_{i+2}}} + \frac{V_L P_{i+2}}{P_{i+2} + P_L} \rho \right) \right]$$

$$G_{i+2} - G_{i+3} = \dots\dots\dots$$

$$G_{i+3} - G_{i+4} = \dots\dots\dots \quad (2)$$

Results of volumetric balance calculations and the drainage area determined based on these calculations indicated that the radii of drainage varied between 362 m and 455 m for GGVs (Table 4). These numbers indicate that strata deformations in terms of stress-relief fracturing and bedding plane separations exceed panel widths—in accordance with Gale<sup>23</sup> who demonstrated that horizontal conductivity, which is enhanced through bedding plane separations—can be beyond panel dimensions. Calculated radii of drainage of GGVs also indicate that they can slightly overlap between GGVs. It should be kept in mind, however, that these radii are the maximum distances beyond which any event would not be observed during GGV production. Therefore, following the PSS concept, these distances can be considered as the maximum physical extents of the deformation boundary determined by using the available data, which is of relevance for gas availability and flow for GGVs. Although the calculated radius of drainage gives an approximate value and an order of magnitude idea about the true distance for the existence of boundaries, rather than an exact distance,<sup>34</sup> it can be used for GGV spacing design. For similar panels in the Upper Pottsville Formation, for instance, a regular spacing of 700–800 m is reasonable unless there are significant spatial changes in coal properties and the properties of the overburden that may affect stress-relief fracturing and bedding plane separations.

Initial gas-in-place ( $G_i$ ) and gas remaining within the drainage area for each GGV after mining of the E-1 panel was completed ( $G_{E-1 \text{ end}}$ ), and these values are also given in Table 4. These values indicate initial gas amounts ranging between  $12.17 \times 10^6 \text{ m}^3$  and  $19.2 \times 10^6 \text{ m}^3$  within the drainage area of GGVs. At the time of panel completion, methane quantities between  $3.36 \times 10^6 \text{ m}^3$  and  $8.08 \times 10^6 \text{ m}^3$  were still in the drainage area of each GGV to be

captured. These quantities indicate that GGVs were effective in capturing 60%–80% during mining and when dynamic deformations were occurring. These data show the importance of the existence of GGVs and their effectiveness for capturing strata gas during mining and after completion of panels in this area.

The change of gas-in-place computed using Eq. (2) in drainage areas and the cumulative gas captured by the GGVs as a function of time are shown in Fig. 9A and B, respectively. These data show that the gas within the strata available for each GGV decreases significantly with an increase in cumulative gas production especially within the first three months of GGV operation. Considering that this time span corresponds to an average mining distance between 800 and 900 m, which also corroborates the estimated diameters of the drainage areas, these changes may be due to the effects of dynamic subsidence around the boreholes. Fig. 9B further shows that the change in the gradient of the cumulative gas production of GGVs correlates with abrupt changes in face advance rate, when the face is within 800–900 m distance from a particular well location. As the mining face moves away from the GGV location and the effects of dynamic subsidence on strata behavior and hydraulic conductivity diminish, gas-in-place and production seem to change more gradually and are not affected as significantly by the changes in mining rate anymore.

The Pratt group of coal's formation pressure iteratively calculated by Eq. (2) for each well is shown in Fig. 10. This figure shows that stress-relief fracturing and bedding plane separations with subsequent production of high volumes of gas reduce formation pressure from its initially predicted average values of 648 kPa to values on the order of 150 kPa close to the end of mining and after completion of the panel. The data shows that initial rates of pressure declines are generally more significant in each GGV potentially due to the dynamic subsidence around the boreholes. A comparison of Fig. 10 with Fig. 9B also shows that changes in mining rate affect the decline in formation pressure the same way they do for changes in productivity of the GGVs.

Although pressure decline profiles of each individual GGV location are different, the incremental gas captured per incremental pressure drop, which can be considered an indication of hydraulic conductivity of the deformed strata, populate along a linear trend, especially for pressure-drop values less than 100 kPa (Fig. 11A and B). These pressure drop values between consecutive dates correspond to almost all phases of GGV production life during mining and after panel completion. At higher pressure drops, the data is more scattered and the relation is more non-linear for some GGVs (16106-CG and 16124-CG) due to the effects of abrupt changes in mining rate on the GGVs. Nevertheless, the data given in Fig. 11A show that the incremental amount of gas that can be captured from this formation by using GGVs as the result of mining disturbances is proportional to the incremental amount of pressure drop by a factor of  $0.0212 (10^6 \text{ m}^3/\text{kPa})$ , and this relation holds linear for the most part and for all GGVs. Although not exact, this relation can be indicative of how much gas capture can be expected from the GGVs during the mining cycle and after panel completion based on the forecasted changes in formation pressure drop.

Before concluding, it should be mentioned that this study is based on the uniform coal properties of the Pratt group and shows consistency between data and analyzed results.

However, it is not uncommon to experience significant spatial changes in the strata gas source. These changes may include variations in coal thickness, and spatial changes in pressure or in coal quality that may affect its gas content. In this case, gas availability and drainage radii of GGVs may be different than the values discussed in this work.

#### 4. Summary and conclusions

This study evaluated gob gas venthole (GGV) performances drilled over a longwall panel operating in Mary Lee/Blue Creek coals to control strata gas originating from the Pratt group of coals in the Upper Pottsville Formation, Alabama. The study showed that the GGVs are highly effective in capturing strata gas from stress-relief fractures and bedding plane separations, and they are shown to be more effective than conventional CBM wells in capturing strata gas for methane control purposes.

Production performances of GGVs show a strong apparent correlation between mining rate and methane production rates. This signifies the importance of mining rate on dynamic subsidence and associated methane release from gassy strata, as well as the enhancement of hydraulic conductivity around gob gas boreholes to capture it more effectively. This also indicates that, if there are no GGVs ready to capture the strata gas, slowing mining advance may help to reduce gas emitted from strata to aid in ventilation.

Volumetric gas in-place assessment was performed to estimate drainage area of each GGV, as well as changes in formation pressures and in-place gas contents. These calculations showed that the radii of drainage varied between 362 m and 455 m for GGVs. These numbers indicate that strata deformations in terms of stress-relief fracturing and bedding plane separations exceed panel widths and are slightly overlapping between GGVs, and can be used as a guide for GGV placement spacing. Based on these values, a regular spacing of 700–800 m is reasonable for this area.

As for the depth of the GGVs, the source of gas in this geology is considered as the Pratt group of coals. Present completion designs of GGVs cover the entire gas source and flow interval. However, although there is no data to support this assertion, a slotted casing, at least through the main Pratt coals at the top, may help to stabilize the borehole and may help to improve the productivity.

Initial gas-in-place and gas remaining within the drainage area for each GGV after mining of the E-1 panel indicated initial gas amounts ranging between  $12.17 \times 10^6 \text{ m}^3$  and  $19.2 \times 10^6 \text{ m}^3$  within the drainage area of GGVs. At the time of panel completion, 60–80% of these quantities were already captured, showing the importance of GGVs for capturing strata gas during mining.

Calculated formation pressures decreased significantly within the strata as a result of fracturing and gas production. However, the gradient of gas production and pressure decline is affected by changes in mining rates, if the face is still within the drainage area of the GGV.

There is an approximate linear relationship between incremental pressure drop and incremental gas production in this field. The proportionality constant is  $0.0212 (10^6 \text{ m}^3/\text{KPa})$ .

## References

1. Diamond, WP. Methane Control for Underground Coal Mines. US Bureau of Mines Information Circular No. 9395; Pittsburgh, PA: 1994.
2. Karacan CÖ, Ruiz FA, Cotè M, Phipps S. Coal mine methane: a review of capture and utilization practices with benefits to mining safety and to greenhouse gas reduction. *Int J Coal Geol.* 2001; 86:121–156.
3. Schatzel SJ, Karacan CÖ, Dougherty HN, Goodman GVR. An analysis of reservoir conditions and responses in longwall panel overburden during mining and its effect on gob gas well performance. *Eng Geol.* 2012; 127:65–74.
4. Sang S, Xu H, Fang L, Li G, Huang H. Stress relief coalbed methane drainage by surface vertical wells in China. *Int J Coal Geol.* 2010; 82:196–203.
5. Karacan CÖ, Goodman GVR. Probabilistic modeling using bivariate normal distributions for identification of flow and displacement intervals in longwall overburden. *Int J Rock Mech Min Sci.* 2011; 48:27–41.
6. Yang TH, Xua T, Liu HY, Tang CA, Shi BM, Yu QX. Stress-damage-flow coupling model and its application to pressure relief coal bed methane in deep coal seam. *Int J Coal Geol.* 2011; 86:357–366.
7. Szl zak N, Obracaj D, Swolkie J. Methane drainage from roof strata using an overlying drainage gallery. *Int J Coal Geol.* 2014; 136:99–115.
8. Kong S, Cheng Y, Ren T, Liu H. A sequential approach to control gas for the extraction of multi-gassy coal seams from traditional gas well drainage to mining-induced stress relief. *Appl Energy.* 2014; 131:67–78.
9. Chen J, Wang T, Zhou Y, Zhu Y, Wang X. Failure modes of the surface venthole casing during longwall coal extraction: a case study. *Int J Coal Geol.* 2012; 90–91:135–148.
10. Liang S, Elsworth D, Li X, Yang D. Topographic influence on stability for gas wells penetrating longwall mining areas. *Int J Coal Geol.* 2014; 132:23–36.
11. Karacan CÖ. Forecasting gob gas venthole production performances using intelligent computing methods for optimum methane control in longwall coal mines. *Int J Coal Geol.* 2009; 79:131–144.
12. Karacan CÖ, Olea RA. Sequential Gaussian co-simulation of rate decline parameters of longwall gob gas ventholes. *Int J Rock Mech Min Sci.* 2013; 59:1–14.
13. Liu Q, Cheng Y, Yuan L, Tong B, Kong S, Zhang R. CMM capture engineering challenges and characteristics of in-situ stress distribution in deep level of Huainan coalfield. *J Nat Gas Sci Eng.* 2014; 20:328–336.
14. Palchik V. Formation of fractured zones in overburden due to longwall mining. *Environ Geol.* 2003; 44:28–38.
15. Palchik V. Localization of mining-induced horizontal fractures along rock layer interfaces in overburden: field measurements and prediction. *Environ Geol.* 2005; 48:68–80.
16. Whittles DN, Lowndes IS, Kingman SW, Yates C, Jobling S. Influence of geotechnical factors on gas flow experienced in a UK longwall coal mine panel. *Int J Rock Mech Min Sci.* 2006; 43:369–387.
17. Karacan CÖ, Olea RA. Inference of strata separation and gas emission paths in longwall overburden using continuous wavelet transform of well logs and geostatistical simulation. *J Appl Geophys.* 2014; 105:147–158.
18. Guo H, Yuan L, Shen B, Qua Q, Xue J. Mining induced strata stress changes, fractures and gas flow dynamics in multi-seam longwall mining. *Int J Rock Mech Min Sci.* 2012; 54:129–139.
19. Karacan CÖ, Goodman GVR. Monte Carlo simulation and well testing applied in evaluating reservoir properties in a deforming longwall overburden. *Transp Porous Media.* 2011; 86:445–464.

20. Karacan CÖ. Reconciling longwall gob gas reservoirs and venthole production performances using multiple-rate drawdown well test analysis. *Int J Coal Geol.* 2009; 80:181–195.
21. Adhikary DP, Guo H. Modelling of longwall mining-induced strata permeability change. *Rock Mech Rock Eng.* 2015; 48:345–359.
22. Karacan CÖ, Goodman G. Hydraulic conductivity and influencing factors in longwall overburden determined by using slug tests in gob gas ventholes. *Int J Rock Mech Min Sci.* 2009; 46(7):1162–1174.
23. Gale, W. Proceedings of the Coal2005, 6th Australasian Coal Operator's Conference. Brisbane, Australia: 2005. Application of computer modeling in the understanding of caving and induced hydraulic conductivity about longwall panels.
24. Pashin JC. Hydrodynamics of coalbed methane reservoirs in the Black Warrior Basin: key to understanding reservoir performance and environmental issues. *Appl Geochem.* 2007; 22:2257–2272.
25. Groshong RH, Pashin JC, McIntyre MR. Structural controls on fractured coal reservoirs in the southern Appalachian Black Warrior foreland basin. *J Struct Geol.* 2009; 31:874–886.
26. Pashin JC. Variable gas saturation in coalbed methane reservoirs of the Black Warrior Basin: implications for exploration and production. *Int J Coal Geol.* 2010; 82:135–146.
27. Karacan CÖ. Production history matching to determine reservoir properties of important coal groups in Upper Pottsville formation, Brookwood and Oak Grove fields, Black Warrior Basin, Alabama. *J Natur Gas Sci Eng.* 2013; 10:51–67. [PubMed: 26191096]
28. Karacan CÖ, Olea RA. Time-lapse analysis of methane quantity in Mary Lee group of coal seams using filter-based multiple-point geostatistical simulation. *Math Geosci.* 2013; 45:681–704. [PubMed: 26191095]
29. Karacan CÖ. Integration of vertical and in-seam horizontal well production analysis and stochastic geostatistical algorithms to estimate pre-mining methane drainage efficiency from coal seams: Blue Creek seam, Alabama. *Int J Coal Geol.* 2013; 114:96–113. [PubMed: 26435557]
30. Preusse, A. Proceedings Of 20th International Conference on Ground Control in Mining. Morgantown, WV: 2001. Effect of face advance rates on the characteristics of subsidence processes associated with US and Germany longwall mining.
31. Karacan, CÖ., Diamond, WP., Esterhuizen, GS., Schatzel, SJ. Proceedings of the 2005 International Coalbed Methane Symposium. Tuscaloosa, Alabama: May 17–19. 2005 Numerical analysis of the impact of longwall panel width on methane emissions and performance of gob gas ventholes.
32. Suchowerska AM, Merifield RS, Carter JP. Vertical stress changes in multi-seam mining under supercritical longwall panels. *Int J Rock Mech Min Sci.* 2013; 61:306–320.
33. Mazza RL, Mlinar MP. Reducing methane in coal mine gob areas with vertical boreholes. US Bureau of Mines Research Report 1607-1. 1977:77.
34. Oliver DS. The averaging process in permeability estimation from well-test data. *SPE Form Eval.* 1990; 5(3):319–324.



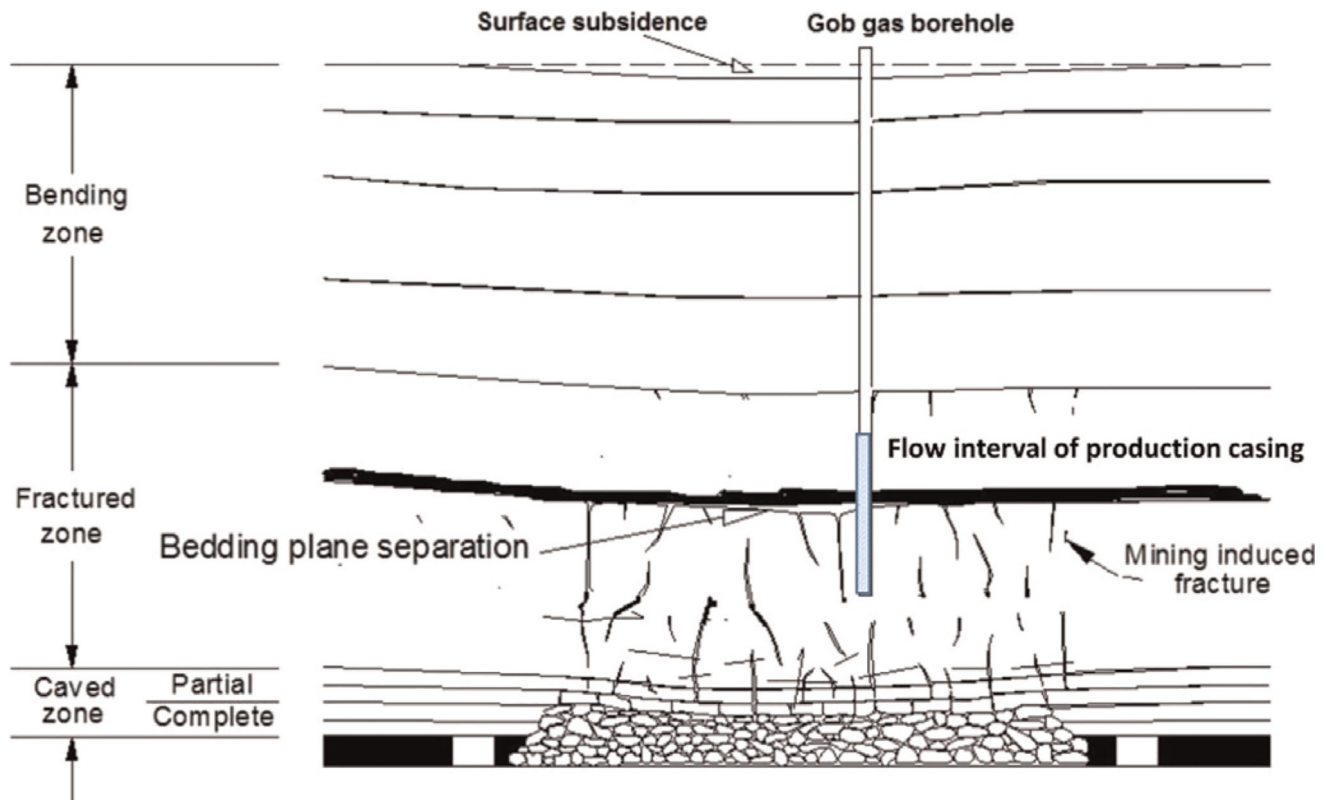


**Fig. 1.**

A schematic representation of deformed overburden as a response to longwall mining, and location of GGV to control strata gas.

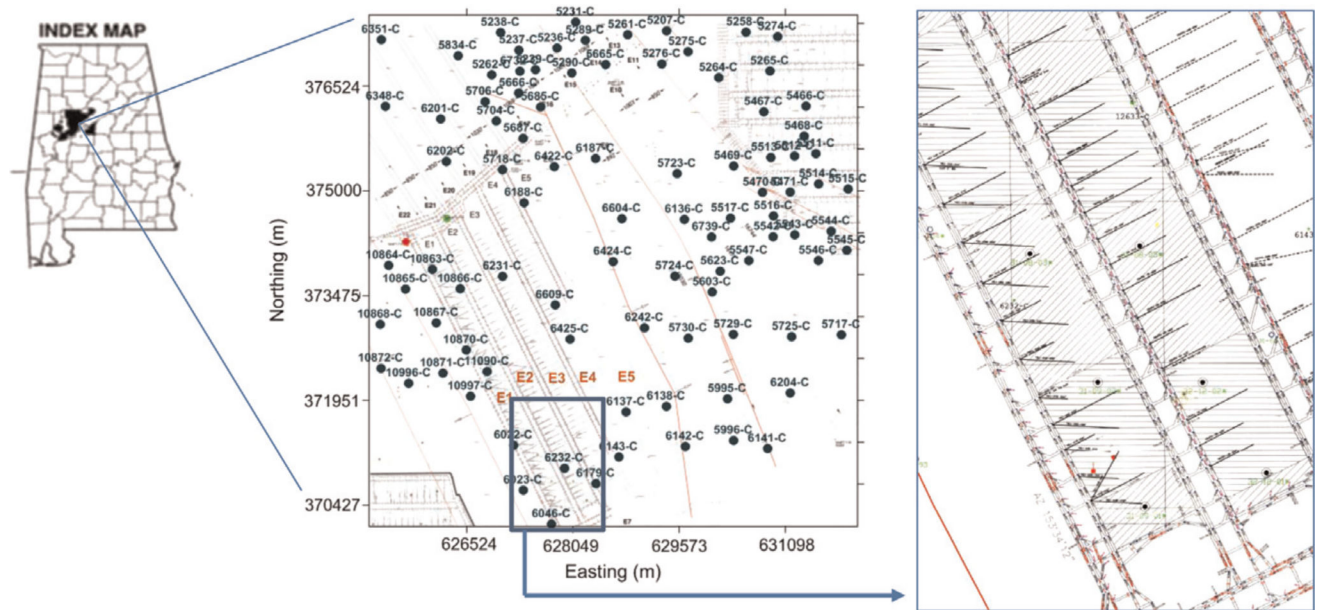


**Fig. 2.**

Location of study area and a plan view with vertical degasification wellbore locations, mine outline, and major geologic structures with vertical displacements. The figure on the right is an expanded section of the panels that shows the horizontal, in-seam degasification boreholes.

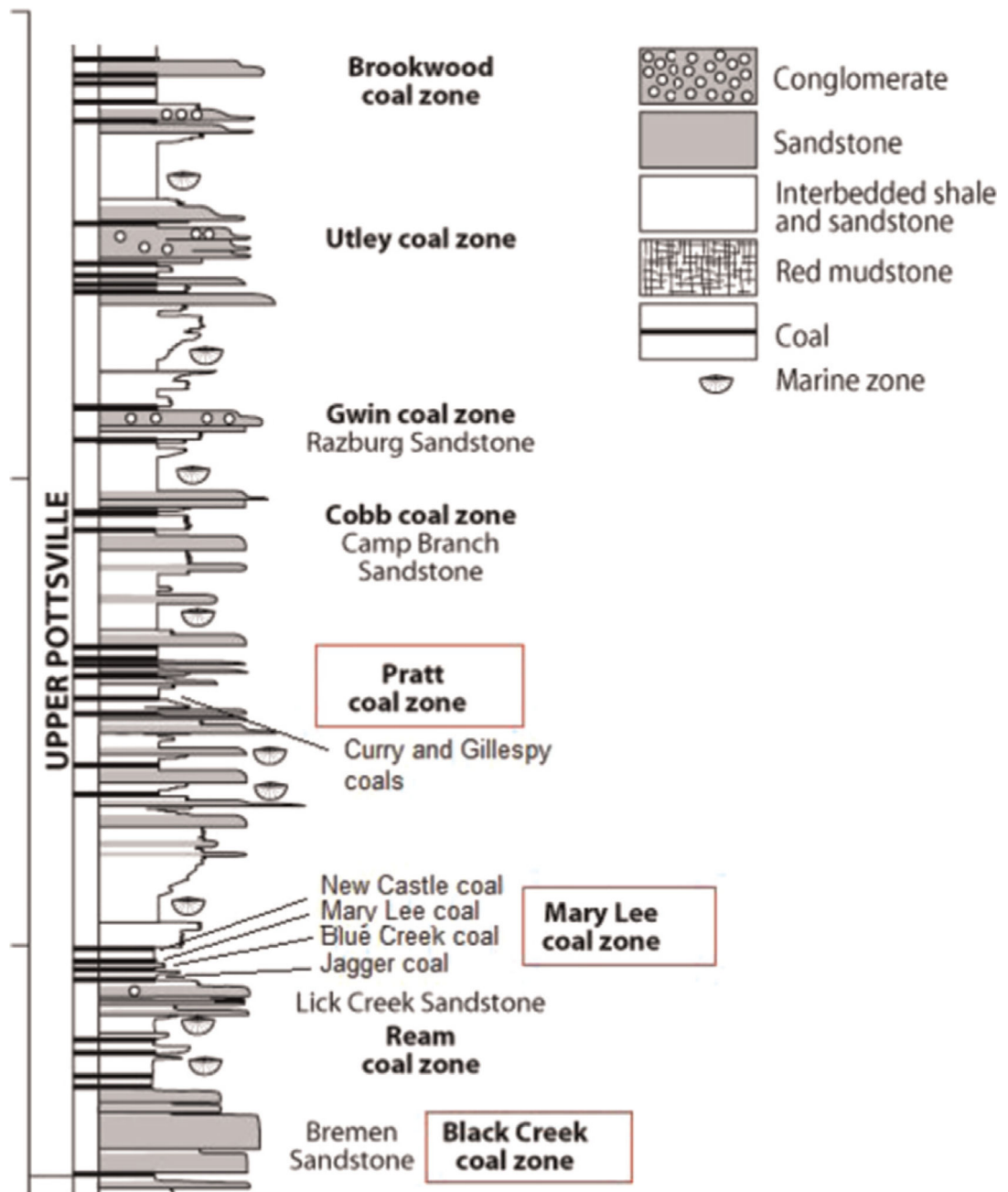


**Fig. 3.**  
Stratigraphic section of the Upper Pottsville Formation in the Black Warrior basin.

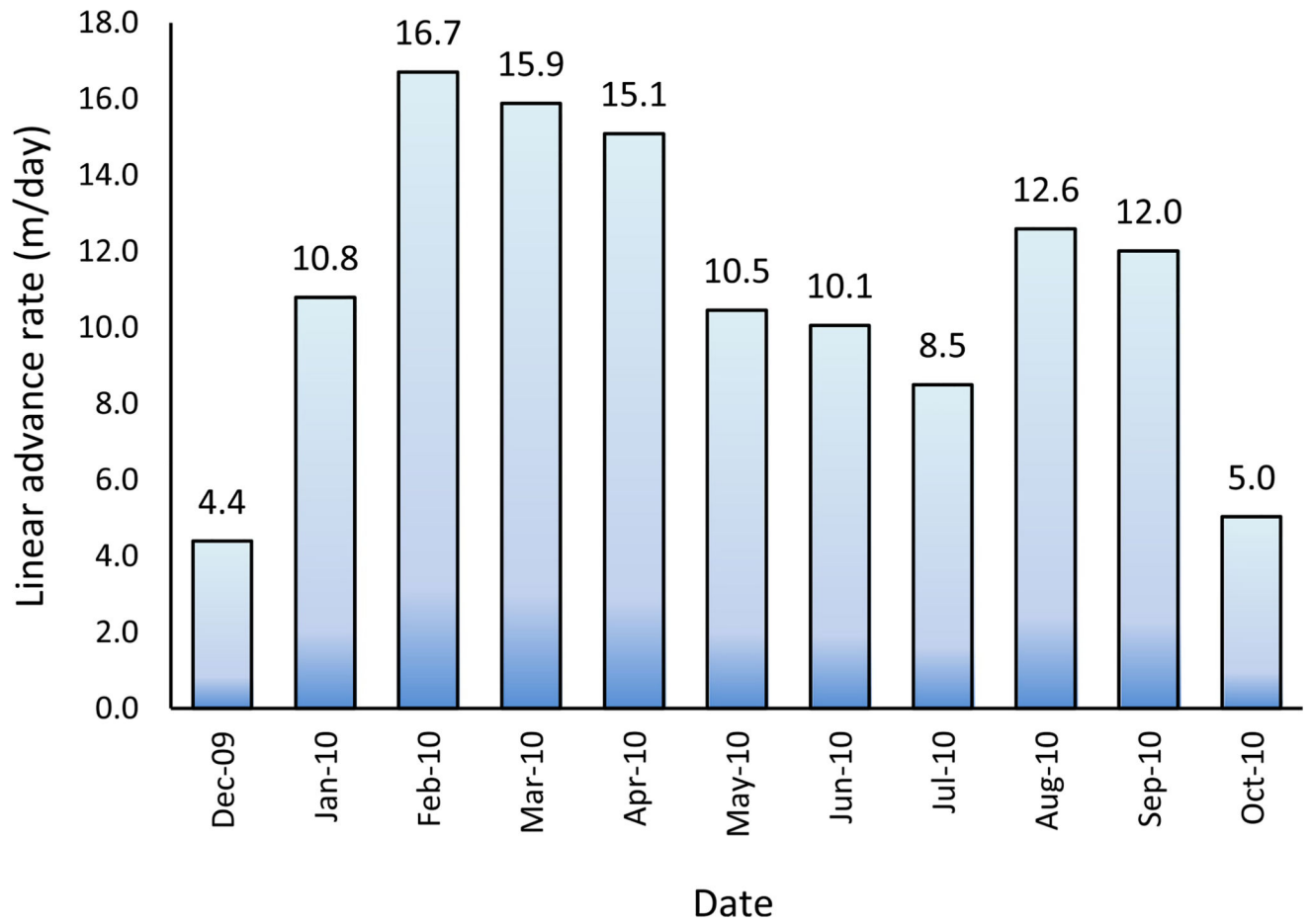


**Fig. 4.**  
Monthly averaged daily advance rate of the longwall face while mining the E-1 panel.

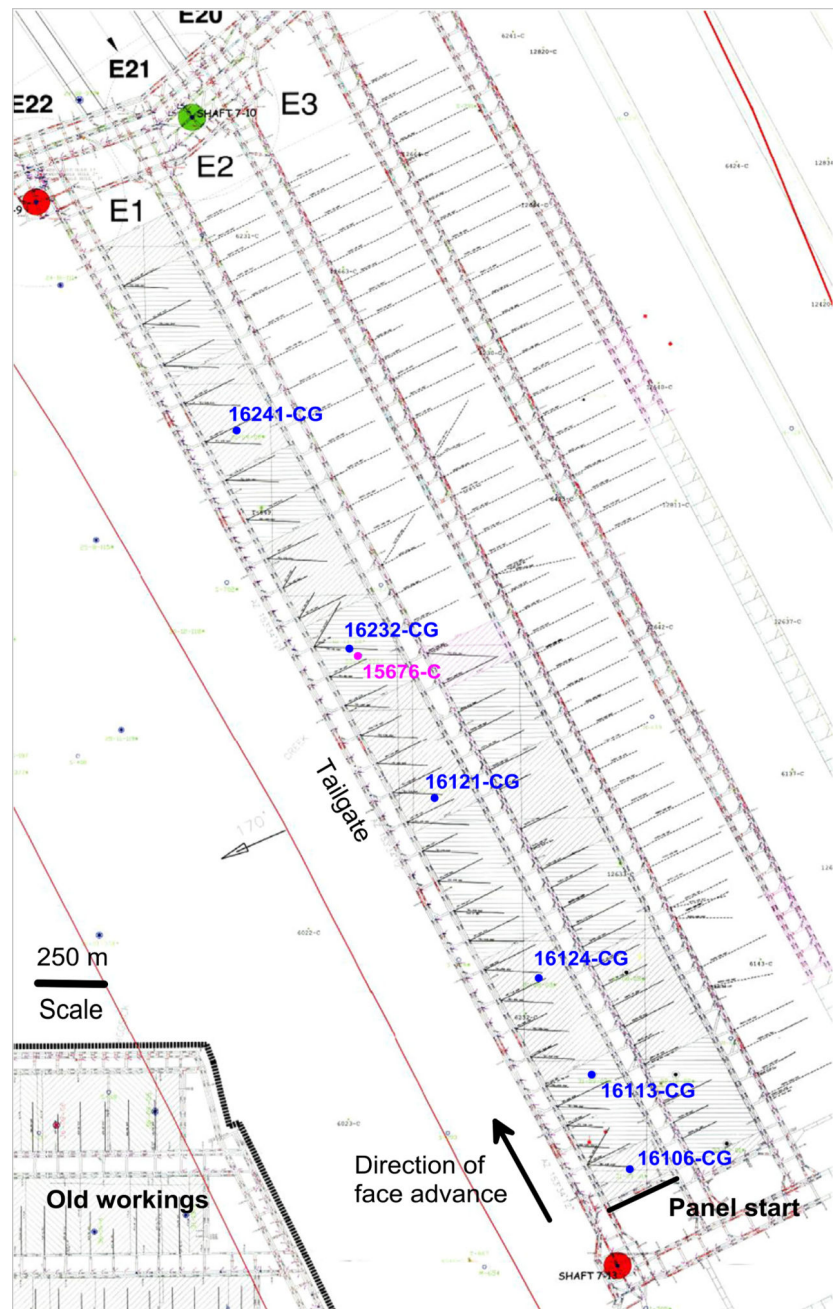


**Fig. 5.**  
Detailed map of the mine, the E-1 panel layout, and locations of the GGVs.

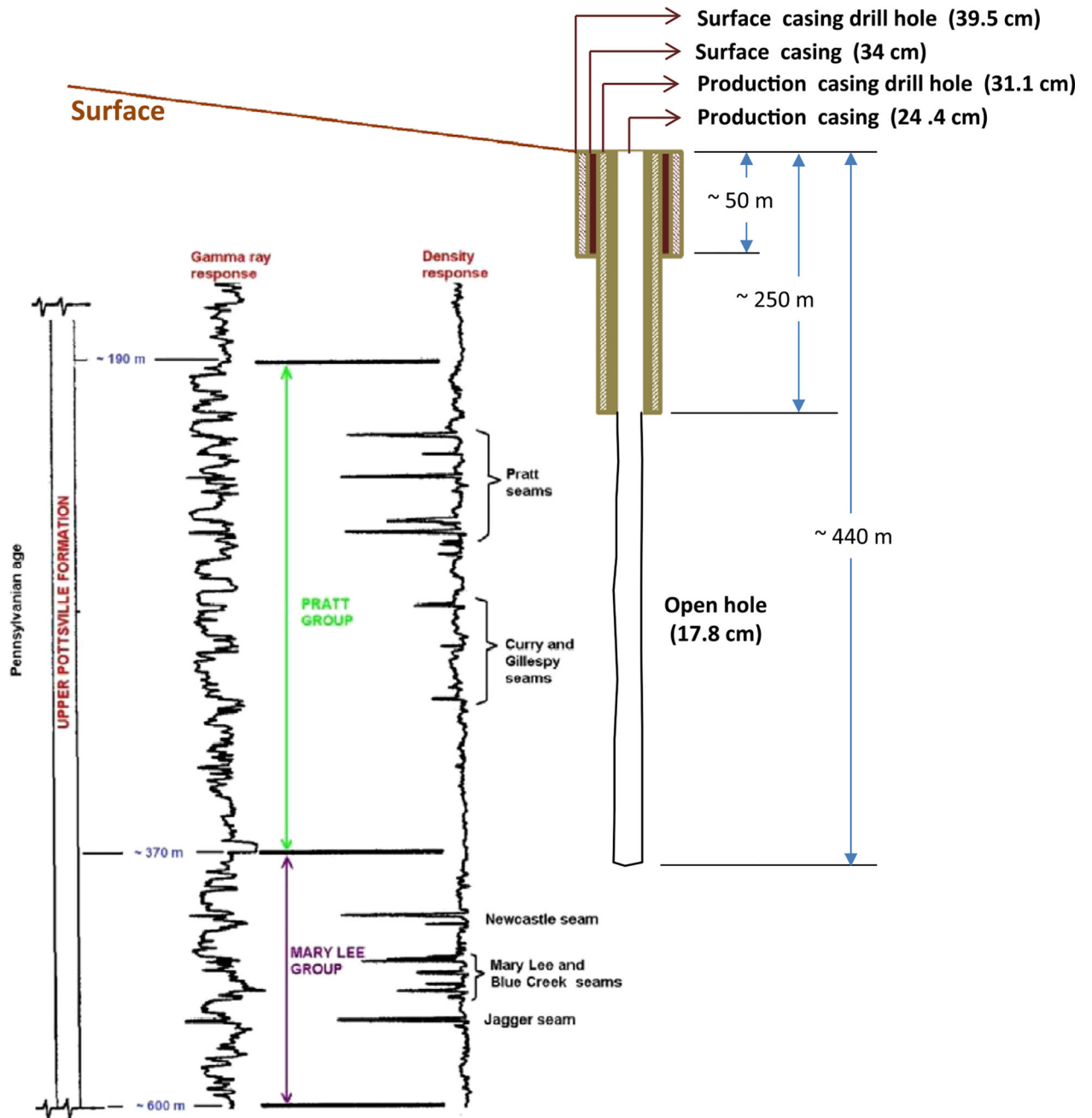


**Fig. 6.**  
Well design specifications of the GGVs used at the mine site and the completion intervals.  
The numbers in parentheses are diameters.



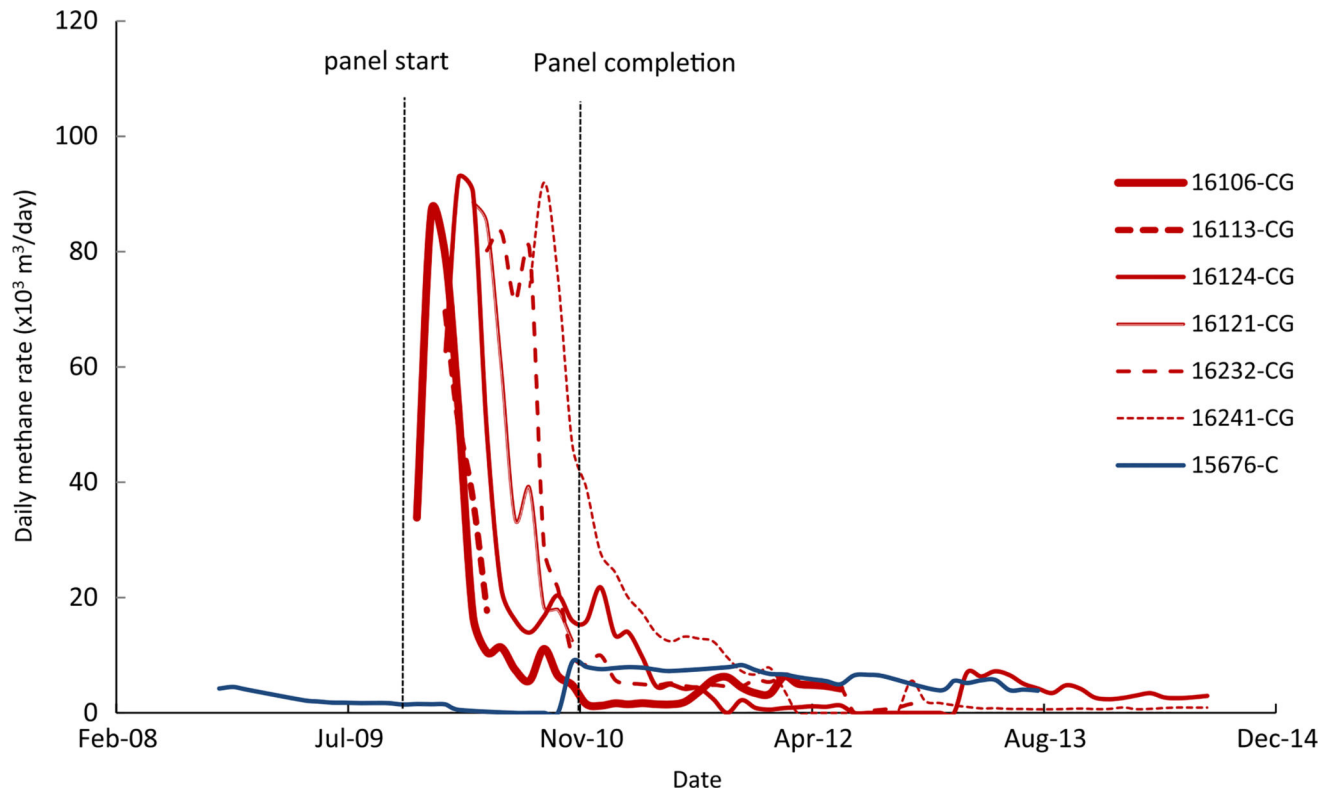


**Fig. 7.**  
Methane production profiles of GGVs during and after mining of the E-1 panel.

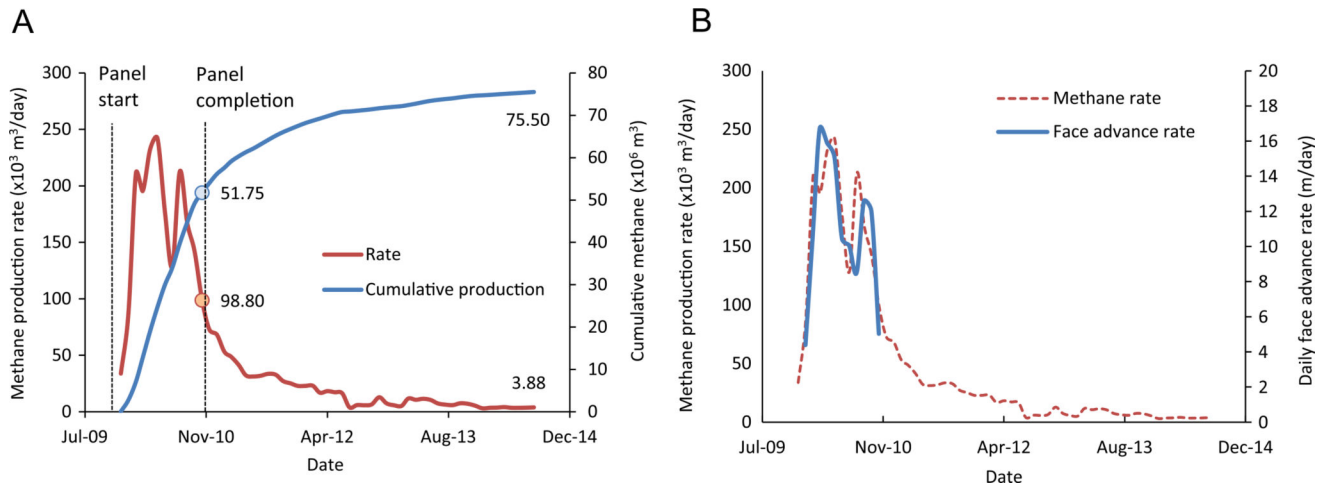


**Fig. 8.** Rate and cumulative methane production from all GGVs (a) and the correlation of mining advance rate to methane production rate (B).

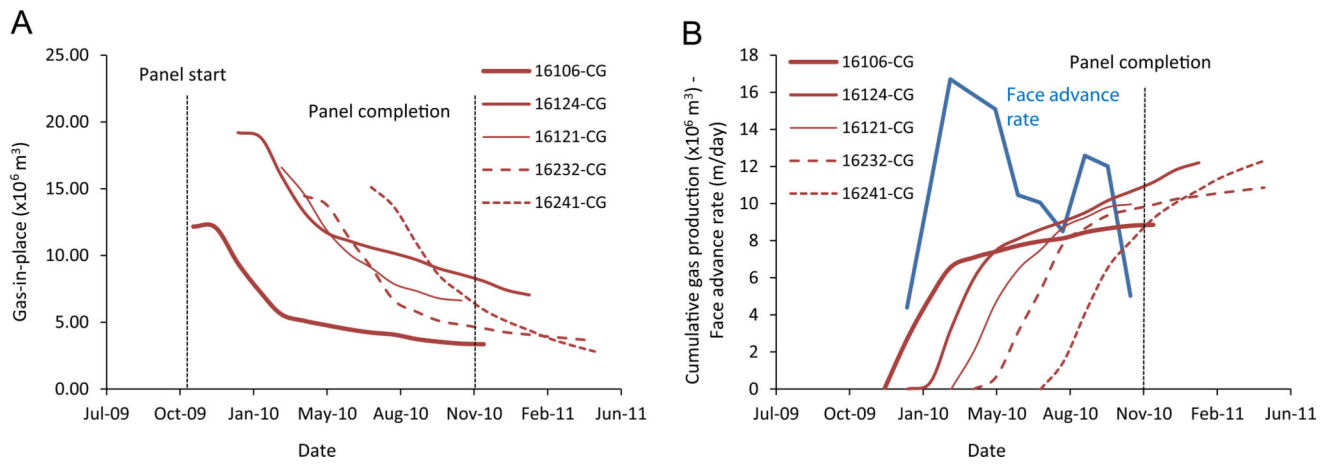


**Fig. 9.**

Change in gas-in-place with time within the drainage area of each GGV (A), and cumulative gas productions from these wells during the same duration (B).

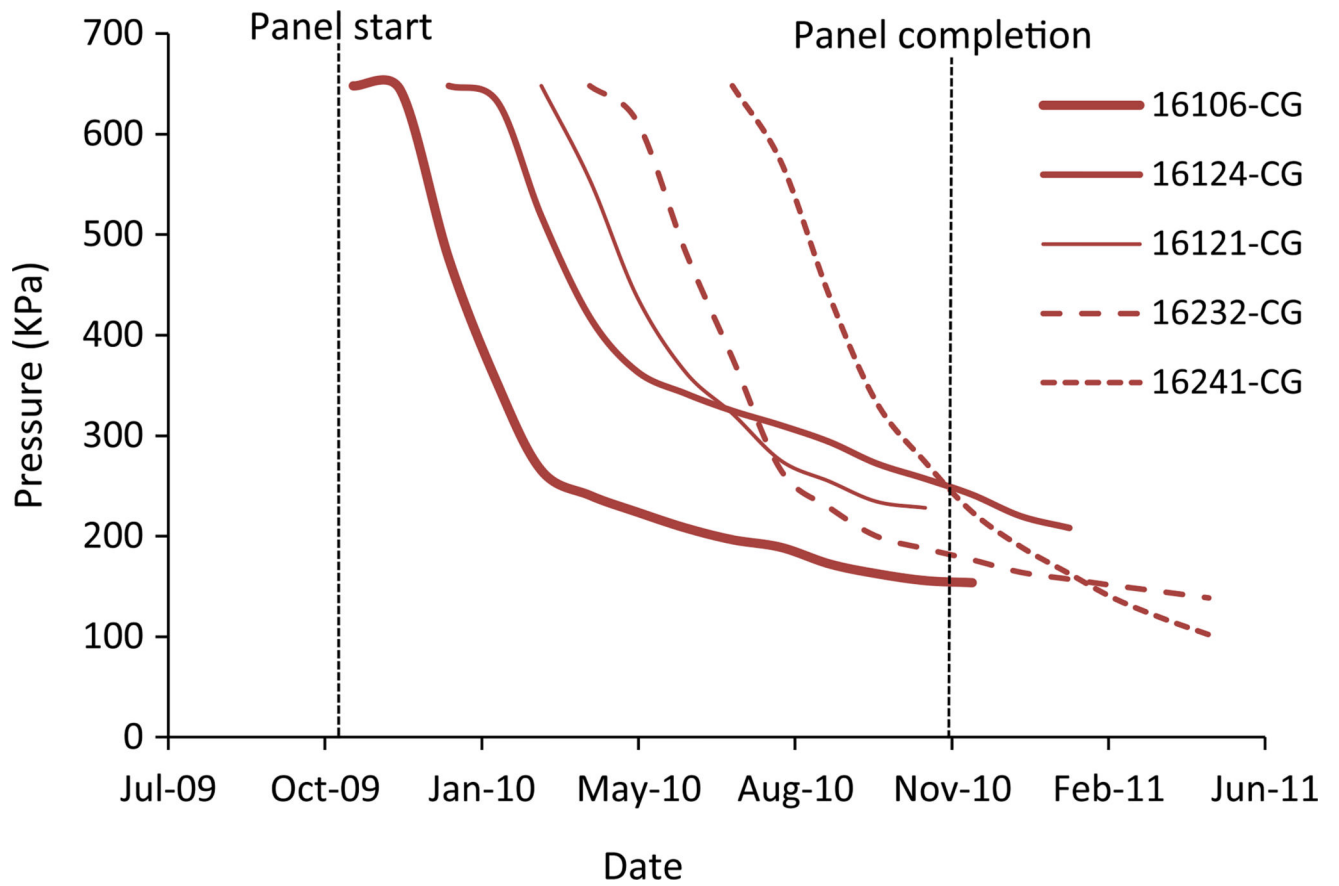


**Fig. 10.**  
Pressure change in the deformed coal strata due to gas production from GGVs.

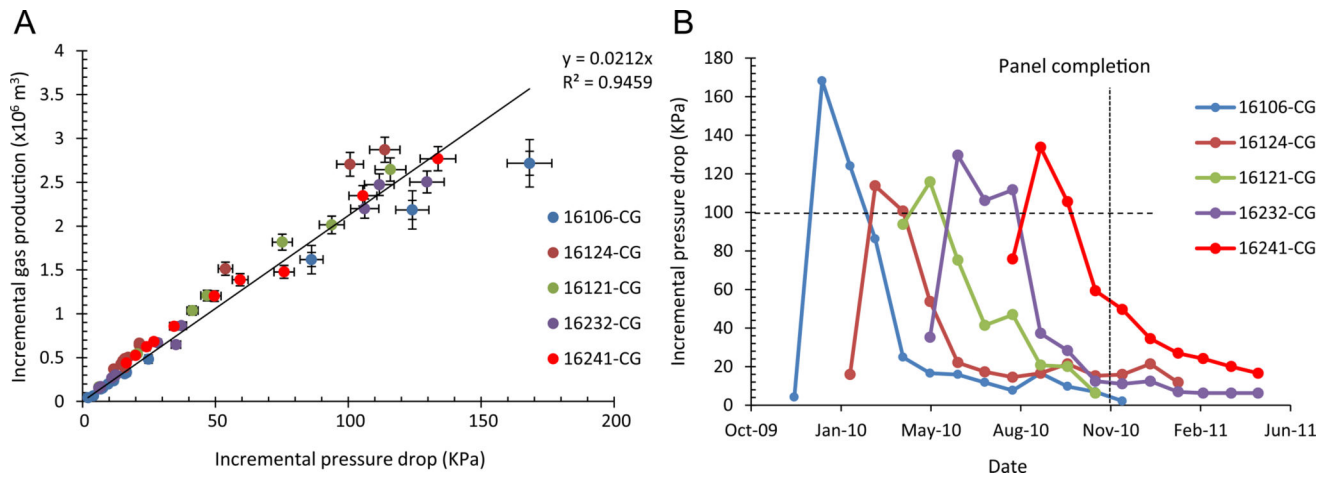


**Fig. 11.** Incremental gas production and formation pressure drop relation (A) and the history of change in pressure drop (B) during mining of the E-1 panel. The error bars in 10-A show 10% error margin of the value of the data points, whereas the 100 KPa level in B show the limit up to which the relation is linear for all GGVs.

**Table 1**

GGVs, their locations on the E-1 panel, and completion details.

Permit	Distance from panel start (m)	Distance from tail-gate (m)	Total depth (m)	Surface elevation (m)	Surface casing setting depth (m)	Production casing setting depth (m)	Open hole interval (m)
16106-CG	72	120	431	177	46	279	152
16113-CG	410	150	442	186	48	295	147
16124-CG	792	144	433	166	37	278	155
16121-CG	1500	114	431	156	47	271	160
16232-CG	2083	105	434	142	47	252	183
16241-CG	2930	105	442	161	47	261	181
15676-C	2040	130	760	142	107	724	-



**Table 2**

Flow tests conducted on the E-1 panel GGVs and their results.

Permit	Test date	Flow ( $\times 10^3$ m <sup>3</sup> /day)	Pressure (KPa)
16106-CG	8-Jul-10	45.7	206.8
16113-CG	-	53.3	315.1
16124-CG	14-Jul-10	40.5	342.6
16121-CG	14-Jul-10	37.7	363.3
16232-CG	13-Jul-10	54.9	377.1
16241-CG	13-Sep-10	26.2	273.7
15676- C	16-Feb-09	3.8	-

**Table 3**

Basic average coal properties at the start of the E-1 panel.

Definition	Parameter	Value
Average initial water saturation	$\bar{S}_w = S_{wi}$	0.56
Average initial coal cleat porosity	$\bar{\phi} = \phi_i$	0.015
Langmuir volume, as received	$V_L$ (m <sup>3</sup> /ton)	19.1
Langmuir pressure, as received	$P_L$ (KPa)	2861
Average initial coal pressure	$\bar{P} = P_i$ (KPa)	648
Coal density, bulk	$\rho$ (ton/m <sup>3</sup> )	1.45
Coal thickness	$h$ (m)	5.2

**Table 4**

Calculated drainage radii and in-place gas amounts initially and at the time of completion of the E-1 panel.

Permit	$r_e$ (m)	$G_i (\times 10^6 \text{ m}^3)$	$G_{E-1 \text{ end}} (\times 10^6 \text{ m}^3)$
16106-CG	362	12.17	3.36
16113-CG	-	-	-
16124-CG	455	19.20	8.08
16121-CG	423	16.59	6.63
16232-CG	395	16.47	4.55
16241-CG	403	15.12	5.94